NUCLEAR SCIENCE AND TECHNIQUES **26**, 040501 (2015)

Simulation of (p,d) reaction on RIBLL2 for study of tensor force*

GUO Chen-Lei (郭晨雷),[1,2,3] ZHANG Gao-Long (张高龙),[1,2,3,†] QU Wei-Wei (屈卫卫),[2,3]
Satoru Terashima,[2,3] Isao Tanihata,[2,3,4] and LE Xiao-Yun (乐小云)[2,3]

[1]*State Key Laboratory of Software Development Environment, Beihang University, Beijing 100191, China*
[2]*School of Physics and Nuclear Energy Engineering, Beihang University, Beijing 100191, China*
[3]*International Research Center for Nuclei and Particles in the Cosmos, Beihang University, Beijing 100191, China*
[4]*Research Center for Nuclear Physics, Osaka University, Osaka 567-0047, Japan*

(Received December 29, 2014; accepted in revised form February 13, 2015; published online August 20, 2015)

In order to study the effect of tensor force, we plan to perform a (p,d) reaction with a 400–1600 MeV proton beam on the RIBLL2 at Lanzhou. Based on the experimental conditions of RIBLL2, a Monte Carlo method is used to simulate (p,d) reaction process. The distributions of primary beam and scattered deuterons are given on the target and at the F_1, F_2, F_3, and F_4 positions. Considering the yield of the deuteron, to separate the produced deuteron from the background particles, the target thickness is optimized. To obtain a clear particle identification spectrum by time of flight (*TOF*) and energy loss (ΔE), the distance between the two detectors, as well as the energy and timing resolution of detectors are simulated. As a result, the distance between F_2 and F_4 is fit for that of *TOF*. After taking into account the particle distribution at F_4, both sizes of Multi-Wire Drift Chamber, namely MWDC2 and MWDC3, are selected to be 50 mm × 50 mm.

Keywords: Tensor force, Monte Carlo simulation, RIBLL2

DOI: 10.13538/j.1001-8042/nst.26.040501

I. INTRODUCTION

Tensor forces play an important role in the pion exchange interactions that provide the most important attraction in nuclear forces [1–3]. The importance of the tensor forces has been demonstrated to reproduce the properties of nuclear matter, as well as explain the binding energy [4] of deuteron and alpha particles. Admixture of D-wave in those nuclei provides clear evidence of the tensor interactions [5]. Recently, theoretical calculations on $^{9-11}$Li that include explicitly the tensor interactions have pointed out [6] the importance of the tensor interactions in understanding the structure of those nuclei to predict high momentum components in ground states.

Experiments using the electron [7, 8] or proton-induced [9] knockout reaction have been performed to probe the tensor correlations in nuclei from ^{12}C to ^{208}Pb. However, due to other correlations such as short-range repulsion, it is difficult to isolate the tensor effects unambiguously in these experiments.

In fact, theoretical calculations [1, 3, 10] have predicted enhanced momentum distributions at around 2 fm^{-1} due to the tensor interactions, mixing large orbital angular momentum states through the D-wave. The 2 fm^{-1} has ∼400 MeV/c momentum transfer and corresponds to a 800 MeV proton beam.

We aim to explore the effects of tensor force on ^{16}O nucleus. In the shell model, the ground state of ^{16}O consists of eight protons and eight neutrons filling up the $1s_{1/2}$, $1p_{3/2}$ and $1p_{1/2}$ orbits. Since the tensor interactions induce changes in the total orbital and spin angular momenta by $|\Delta L| = 2$ and $|\Delta S| = 2$, the positive-parity states of ^{15}O can be reached through direct one-neutron pick-up reaction, only if the ^{16}O ground state has an admixture of $1d_{5/2}$ and $2s_{1/2}$ in the absence of multi-step process. Although other residual central interactions may also mix in such states, the mixed wave function from the tensor interactions is expected to have high-momentum components that are more significant than the others.

We will measure the differential cross sections of (p,d) reactions on ^{16}O. The advantage of this reaction lies in the selectivity of the momentum of the picked-up neutron. Combined with previous accomplished and acquired experimental data [11–13], we would like to see the different behavior of the cross sections on the internal momentum of the picked-up neutron due to the effect of the tensor interactions. (p,d) reaction cross sections at 0° are measured for the transition to the normal parity states, as well as to the abnormal parity state. Examples are the ^{16}O(p, d)^{15}O(gs $\frac{1}{2}^-$) and ^{16}O(p, d)^{15}O(6.2 MeV $\frac{3}{2}^-$) as normal parity transitions and ^{16}O (p,d)^{15}O(5.2 MeV $\frac{1}{2}^+$) as an abnormal parity transition. The effect of tensor force on the momentum distribution is expected to appear strongly in an abnormal parity transition. Therefore, the comparison of the energy dependence of the cross sections of those transitions can provide clear evidence of the tensor forces. Due to the large high momentum amplitude resulting from the tensor forces, the ratio of the cross section of abnormal parity state to the normal parity state would increase.

Previous experiments were performed in RCNP WS-beamline at Osaka university [13]. We already observed a marked enhancement in the ratio for the $\frac{1}{2}^+$ and/or $\frac{5}{2}^+$ state(s) in ^{15}O. However, because of the energy limit in RCNP

* Supported by National Natural Science Foundation of China (Nos.11475013, 11035007 and 11175011), State Key Laboratory of Software Development Environment (No. SKLSDE-2014ZX-08) as well as Fundamental Research Funds for the Central Universities and the Key Laboratory of High Precision Nuclear Spectroscopy, Institute of Modern Physics, Chinese Academy of Sciences
† Corresponding author, zgl@buaa.edu.cn

(400 MeV), the experiment has been performed at around 10 degree to cover the required transferred momentum around 2 fm^{-1}. To minimize other reaction mechanisms at 0 degree, we proposed an experiment of 400–1600 MeV/u ^{16}O (p,d)^{15}O reactions at a deuteron angle $\theta_{\rm d} = 0^\circ$ using the RIBLL2 separator at HIRFL.

To obtain the momentum distributions of nucleons in ^{16}O at around 2 fm^{-1}, the proton beam from the CSRm synchrotron should be high quality and its energy range from 400 MeV to 1600 MeV in every 100 MeV step. The proton beam is injected into the target material, either a Carbon plate or ice target (H_2O). We measured the (p,d) reaction for transitions to the ground state and low excited states, as well as the deep *s*-hole state.

II. SIMULATION PROCESS

A. Proton beam and RIBLL2 setting

The proton beam from the CSRm synchrotron should be high quality: the emittance in both directions should be less than 10π mm mrad (3π mm mrad would be the best), the momentum broadening should be less than 0.02%, and the intensity of proton beam should be more than 10^7 particles per period (10^8 if possible). To obtain the momentum distributions of nucleons in ^{12}C and ^{16}O at around 2 fm^{-1}, the incident proton energies will be changed from 400 MeV to 1600 MeV. In Table 1, we show the energy points in this experiment and the momentum transfer from the (p,d) reactions on ^{12}C and ^{16}O at 0°.

TABLE 1. Momentum transfer for (p,d) reactions on ^{12}C and ^{16}O at 0°

$E_{\rm p}$ (MeV)	Momentum transfer (fm^{-1})	
	^{12}C	^{16}O
400	1.50	1.54
500	1.68	1.71
600	1.83	1.86
700	1.96	1.99
800	2.07	2.11
900	2.18	2.21
1000	2.27	2.31
1100	2.35	2.39
1300	2.50	2.54
1600	2.69	2.73

The CSRm and RIBLL2 facilities are shown in Fig. 1. The proton beam, with a beam size around 1 mm, will hit the target at F0, and the RIBLL2 will be run as a 0° spectrometer with a 75 mm (radius) drift. Since the neutron *s*-hole states in ^{12}C and ^{16}O are expected to lie around 25 MeV and the typical width is 10 MeV, we plan to measure excitation energy up to about 40 MeV to cover the *s*-hole states. For this purpose, the slit at the first focal plane of RIBLL2 is set ±6 mm. At this configuration the momentum acceptance of RIBLL2 is ±4%, which can cover the excitation energy up to 40 MeV, even at the lowest proton energy with 400 MeV. Given that the proton will scatter from the edge of the slit, simulation of the multi-scattered proton has been done and only a small amount of the proton will come through the slit. Figure 2 demonstrates the transition of the proton beam and scattered deuteron before the target (upper-left), after the target (upper-right) at F0, after the first quadrupole Q1, before the slit (bottom-left), and after the slit (bottom-right) at F1. By properly setting the magnetic field of Q1, the primary proton beam and scattered deuteron will be separated clearly.

B. Detector system

In this experiment, we will monitor the intensity of the proton beam using a detector system. The four silicon detectors are installed at F0 in the target chamber and detect the light particles produced in the production target. Each silicon detector has a dimension of 30 mm × 30 mm × 0.3 mm. Figure 3 shows a schematic drawing of the beam monitor detectors. Through the counts of four silicon detectors, the position of the primary beam spot on the target can be monitored. The absolute calibration of the intensity can be done by the Faraday cup at the F1 focal plane or by the plastic scintillators at the F2 and F4 focal points. To maintain the vacuum in CSRm, a thin metal foil will be installed to isolate CSRm from RIBLL2. The energy loss and multi-scattered deuterons have been taken into account and simulated.

For the detection and identification of the scattered deuterons from other particles, we use the time of flight (*TOF*) and energy loss (ΔE) method. Figure 4 presents the layout of detectors in this experiment. The *TOF* will be measured by two sets of plastic scintillation detectors (*TOF*1 and *TOF*2) installed at F2 and F4 with a flight distance of 29.3 m. The ΔE will be obtained from the *TOF*2 detectors. All the detectors in Fig. 4 will be placed in the atmosphere. The vacuum of RIBLL2 will be isolated by a 100 μm thick Teijin DuPont film. Energy loss inside the film is negligible. This system allows us to identify protons and deuterons, and provides for separation of excited states in the final nucleus.

The *TOF*1 detectors are made of BC408 plastic scintillators with a dimension of 50 mm × 50 mm × 5 mm. Two Hamamatsu H2431-50 photomultiplier tubes are used to read out signals from both ends. H2431-50 has good time performance: anode rise time is 0.7 ns and transit time is 16 ns. The energy losses in the *TOF*1 detectors for the deuterons in all the experimental cases are about 1–3 MeV, which can produce enough light for the detection of deuterons. The angular spread due to multiple scattering in *TOF*1 is estimated to be less than 2 mrad, which is negligible for our purpose.

The *TOF*2 detectors consist of three BC408 plastic scintillation detector units. Each unit has a dimension 300 mm × 100 mm × 10 mm and is viewed by two Hamamatsu H2431-50 photomultiplier tubes. The *TOF*2 detectors have an active area of 300 mm × 300 mm. The large area is chosen to meet the beam spot requirement. The *TOF* vs. ΔE spectrum for the ^{16}O (p,d)^{15}O reaction at an incident proton energy of 400 MeV has been simulated and shown in Fig. 5(a). In the simulation, the time resolution of the *TOF*

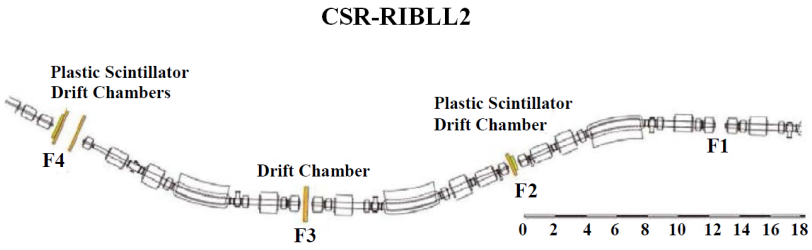

Fig. 1. (Color online) RIBLL2 and experimental setup.

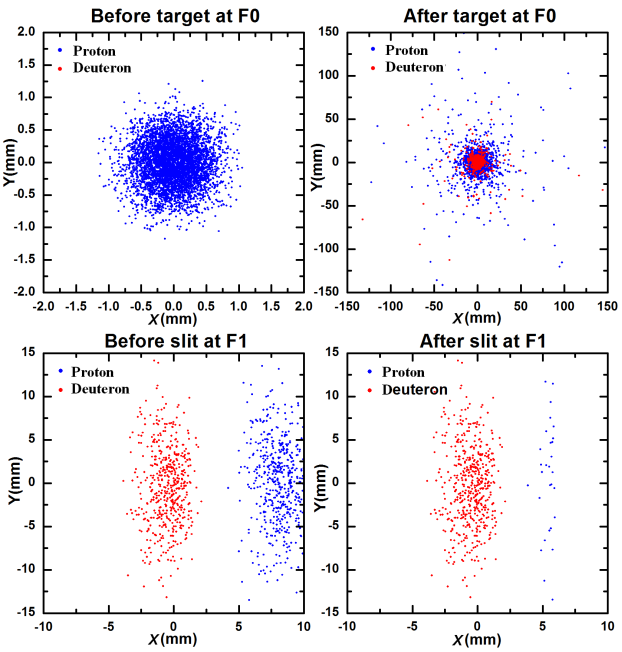

Fig. 2. (color online) The transition of the proton beam and scattered deuteron before the target (upper-left), after the target (upper-right) at F0, before the slit (bottom-left), and after the slit (bottom-right) at F1.

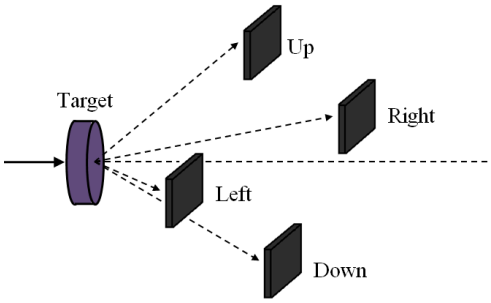

Fig. 3. (Color online) Schematic drawing of the beam monitor detectors.

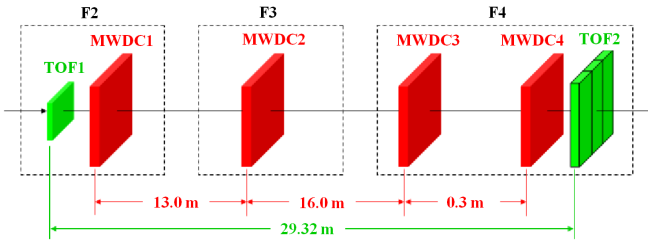

Fig. 4. (Color online) Layout of detectors for deuterons.

detector is 200 ps, the energy resolution of the ΔE detector is 10%, the position resolution of the track detector is 0.4 mm in horizontal and 0.5 mm in vertical, and the excitation energy of ^{15}O is 5.18 MeV and 6.2 MeV. Here we select an ice target (H_2O) with a 0.46 g/cm^2 thickness as the oxygen target, which will be discussed later.

Although the scattered deuterons can be identified from the *TOF* and ΔE method, it is hard to separate the excitation states of ^{11}C and ^{15}O due to the resolutions of the *TOF* and ΔE detectors. If we want to get good resolution of the excitation energy, track detectors (MWDCs) should be used to get precise momentum information of the deuterons. If we put the MWDC1, MWDC2, and MWDC3 at the focus points, according to the ion optics, the momentum P of the deuterons can be calculated by

$$P = B\rho\left(1 + \frac{M_x x_3 - x_2}{D}\right), \quad (1)$$

where $B\rho$, $M_x = -0.48$ and $D = 1.17$ m denote the magnetic rigidity setting, the horizontal magnification, and the dispersion of RIBLL2, respectively [15]. x_2 and x_3 denote the horizontal coordinate of the deuteron measured by MWDC2 and MWDC3, respectively. Figure 5(b) shows the simulation result of the momentum as a function of angles. The angular information of deuterons can be obtained from the position coordinates of MWDC3 and MWDC4. In the simulation, the position resolutions of the drift chambers are 0.4 mm in horizontal and 0.5 mm in vertical, respectively. It is clear that the excitation energy of ^{15}O can be fixed. The focus of this method is that the MWDC1, MWDC2, and MWDC3 must be placed at the focal points; otherwise, the resolutions of momentum spectra get worse. Therefore, the demand for the RIBLL2 beam tuning is quite high.

In this experiment, the active areas of MWDC1, both of MWDC2 and MWDC3, as well as MWDC4 are 150 mm × 150 mm, 300 mm × 300 mm and 480 mm × 320 mm. Each MWDC has six detection planes. In total there are about 740 signals for MWDCs. For the

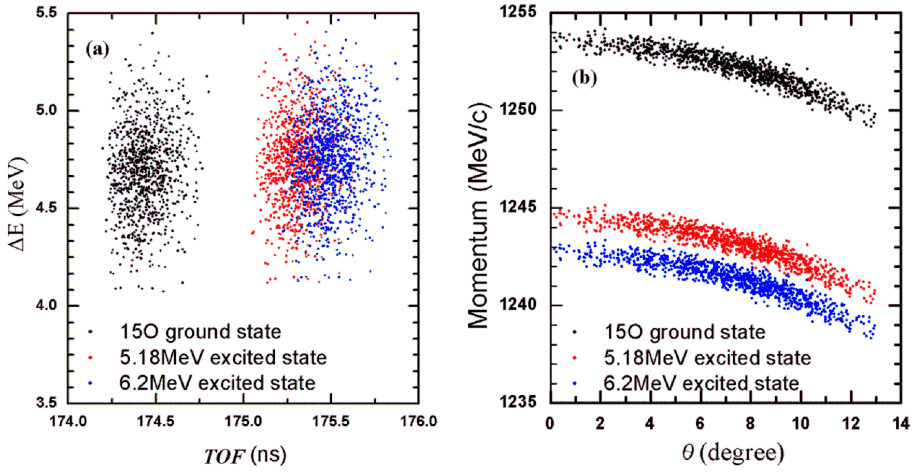

Fig. 5. (color online) The simulated results for the ^{16}O (p,d)^{15}O reaction at an incident proton energy of 400 MeV. (a) Simulated *TOF* vs. ΔE spectrum, (b) simulated Momentum vs. angle spectrum.

read-out of the anode signals and the time digitizing, REPIC RPA-130 preamplifiers and CAEN V1190A TDCs will be utilized. After the time digitizing, the data will be transferred to a computer through a VME crate. In order to obtain precise momentum and angular information, the position resolution of the drift chamber should be better than 0.4 mm in horizontal and 0.5 mm in vertical. The current simulation is based on simple calculations from a few hits with spatial coordinates (X, Y and U), and the set spatial resolution (0.4 mm (X) and 0.5 mm (Y)) is very conservative. A much better spatial resolution ($<$ 250 μm) shall be achievable with the CSR-RIBLL2 gas detectors, as demonstrated in previous published results [15, 16]. The feasibility of Fig. 5 is still on the safe side. Considering the angular resolution and the size of the beam spot at MWDC4, we set a 0.3 m distance between MWDC3 and MWDC4. After taking into account the particle distribution at F4, both of the sizes of MWDC2 and MWDC3 are selected to be 50 mm × 50 mm.

C. Reaction target

An ice target (H_2O) with a 0.46 g/cm^2 thickness will be used in this experiment. The principle of choosing target thickness is to improve the yield ratio of deuteron under the condition of ensuring the resolution of the excitation energy. The effect of the energy loss and multiple scattering of the deuterons in the target at 400 MeV on spectral resolution have been simulated in Eq. (2). The angular distribution of multiple Coulomb scattering is roughly a Gaussian distribution with a width given by

$$\sigma_{\text{M.S.}} = \frac{13.6\text{MeV}}{\beta_c p} z\sqrt{x/X_0}\left[1+0.038\ln\left(\frac{x}{X_0}\right)\right]\text{[rad]}, \quad (2)$$

here p, β_c, and z are the momentum, velocity, and charge number of the incident particles, respectively. x/X_0 is the thickness of the scattering medium in radiation lengths. For the 460 mg/cm^2 ^{16}O target, $\sigma_{\text{M.S.}}$ is about 3 mrad (much less than emittance). On the other hand, the energy straggling caused by multiple scattering increases the momentum spread after the target, as a result, the energy resolution is deteriorated. Figure 5(b) shows the momentum of the produced deuterons as a function of the emission angle. It can be seen that the first two excited states of ^{15}O can be separated well at this thickness.

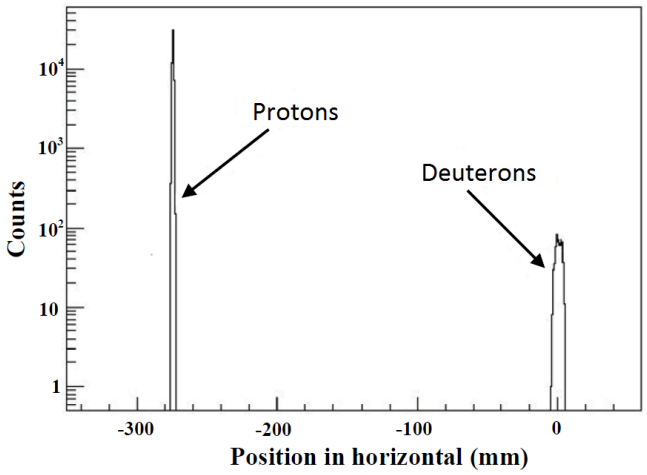

Fig. 6. The F1 simulated horizontal position spectrum of deuterons and scattering protons at a proton energy of 400 MeV.

D. Background consideration

The most likely dominant background in the (p,d) reactions is the elastically scattered protons. However, the momentum of the elastically scattered protons is different from that of the deuterons by about 20% at all incident proton energies. Figure 6 shows the simulation result of the horizontal position

spectrum at F1 of deuterons and scattered protons around 0° at a proton energy of 400 MeV. Since the momentum acceptance of RIBLL2 is set as ±4%, we expect to obtain deuteron spectra free from the proton background.

III. RESULTS AND DISCUSSION

At the proposed scattering angles of the deuterons, the corresponding angles in the CM frame of the d $+^{11}$C or d $+^{15}$O system are smaller than 15°, i.e., larger than 165° in [17]. At this angle, the cross sections for the (p,d) reaction are expected to be in the region of 20 μb/sr to about 100 μb/sr. Assuming the cross section to be ten times smaller than 20 μb/sr, and taking into account the beam intensity ($I = 10^7$ particles per period), the target thickness (g/cm^2), the transfer efficiency of the beam line (ϵ), and the angular acceptance of RIBLL2 ($\Omega = 2.5$ msr), the yields of measured deuterons are estimated as follows

$$Y = \frac{I \times \sigma \times \Omega \times t \times N_{\rm A} \times \epsilon}{M_R}, \qquad (3)$$

where $N_{\rm A}$ is Avogadro number (6.02×10^{23}) and M_R is molecular weight. Before further beam-optic simulation, and based on RIBLL2 beam-line design, we first assumed the transfer efficiency (ϵ) to be 100%, and estimated the time required to obtain about 2000 counts of deuteron events for each energy. The estimated yields and the corresponding running time requirements are summarized in Table 2.

TABLE 2. Estimated yield rates and time requirements

Target	Target thickness (g/cm^2)	Yield (period^{-1})	Time (h)
C	0.45	1.12	100
Ice(H_2O)	0.46	0.77	140

IV. SUMMARY

In order to obtain good energy and angular resolutions, as well as a high production yield for the 400–1600 MeV/u ^{16}O(p,d)^{15}O and ^{12}C(p,d)^{11}C reactions at a deuteron angle $\theta_{\rm d} = 0°$, we used Monte Carlo method to simulate the kinematic process based on the experimental conditions in the HIRFL-RIBLL2 separator. After taking into account target thickness, beam intensity, detector resolution, and so on, the *TOF* and ΔE detector settings were designed and the position and number of MWDCs were simulated. Total beam time and expected cross sections were also estimated. According to software simulation, some hardware conditions, such as beam monitor, high voltage optimization, and background product, need to be considered to achieve the expected results. This method will be continuously explored and developed from the experiment. The effects of tensor force can be systematically studied.

[1] Schiavilla R, Wiringa R B, Pieper S C, *et al*. Tensor forces and the ground-state structure of nuclei. Phys Rev Lett, 2012, **98**: 132501. DOI: 10.1103/PhysRevLett.98.132501

[2] Myo T, Sugimoto S, Kato K, *et al*. Tensor correlation in ^{4}He with the tensor-optimized shell model. Prog Theor Phys, 2007, **117**: 257–274. DOI: 10.1143/PTP.117.257

[3] Neff T and Feldmeier H. Tensor correlations in the unitary correlation operator method. Nucl Phys A, 2003, **713**: 311–371. DOI: 10.1016/S0375-9474(02)01307-6

[4] Bethe H A. The meson theory of nuclear forces, part II. theory of the deuteron. Phys Rev, 1940, **57**: 390–413. DOI: 10.1103/PhysRev.57.390

[5] Ikeda K, Myo T, Kato K, *et al*. Di-neutron clustering and deuteron-like tensor correlation in nuclear structure focusing on ^{11}Li. In: Beck C, editor. Lecture Note in Physics. Springer, 2010, **818**: 165–221. DOI: 10.1007/978-3-642-13899-7_5

[6] Myo T, Kato K, Toki H, *et al*. Roles of tensor and pairing correlations on halo formation in ^{11}Li. Phys Rev C, 2007, **76**: 024350. DOI: 10.1016/S0375-9474(02)01307-6

[7] Piasetzky E, Sargsian M, Frankfurt L, *et al*. Evidence for strong dominance of proton-neutron correlations in nuclei. Phys Rev Lett, 2006, **97**: 162504. DOI: 10.1103/PhysRevLett.97.162504

[8] Leuschner M, Calarco J R, Hersman F W, *et al*. Quasielastic proton knockout from ^{16}O. Phys Rev C, 1994, **49**: 955–967. DOI: 10.1103/PhysRevC.49.955

[9] Yasuda Y, Sakaguchi H, Asajiet S, *et al*. Spectroscopic factors and strength distributions for the deeply bound orbitals in ^{40}Ca obtained from the (p,2p) reaction at 392 MeV. Phys Rev C, 2010, **81**: 044315. DOI: 10.1103/PhysRevC.81.044315

[10] Horiuchi W and Suzuki Y. Momentum distribution and correlation of two-nucleon relative motion in ^{6}He and ^{6}Li. Phys Rev C, 2007, **76**: 024311. DOI: 10.1103/PhysRevC.76.024311

[11] Lee J K P, Mark S K, Portner P M, *et al*. (p,d) reactions on light nuclei at 100 MeV. Nucl Phys A, 1968, **106**: 357–368. DOI:10.1016/0375-9474(67)90880-9

[12] Smith G R, Shepard J R, Boudrie R L, *et al*. (p,d) reaction at 800 MeV. Phys Rev C, 1984, **30**: 593–615. DOI: 10.1103/PhysRevC.30.593

[13] Ong H J, Tanihata I, Tamii A, *et al*. Probing effect of tensor interactions in ^{16}O via (p,d) reaction. Phys Lett B, 2013, **728**: 277–281. DOI: 10.1016/j.physletb.2013.07.038

[14] Sun Z Y, Zhan W L, Guo Z Y, *et al*. RIBLL, the radioactive ion beam line in Lanzhou. Nucl Instrum Meth A, 2003, **503**: 496–503. DOI: 10.1016/S0168-9002(03)01005-2

[15] Yi H, Zhang Z, Xiao Z G, *et al*. Prototype studies on the forward MWDC tracking array of theexternal target experiment at HIRFL-CSR. Chinese Phys C, 2014, **38**: 126002. DOI: 10.1088/1674-1137/38/12/126002

[16] Tang S W, Ma P, Duan L M, *et al*. A normal-pressure MWPC for beam diagnostics at RIBLL2. Chinese Phys C, 2013, **37**: 066002. DOI: 10.1088/1674-1137/37/6/066002

[17] Sekiguchi K, Sakai H, Wita H, *et al*. Resolving the discrepancy of 135 MeV pd elastic scattering cross sections and relativistic effects. Phys Rev Lett, 2005, **95**: 162301. DOI: 10.1103/PhysRevLett.95.162301